Studies on the Growth Control of ZnO Nanostructures synthesized by the Chemical Method

Patricia María Perillo[1], Mariel Nahir Atia[1],
Daniel Fabián Rodríguez[1]

[1]Comisión Nacional de Energía Atómica, Centro Atómico Constituyentes, Depto. Micro y Nanotecnología, Av. Gral. Paz 1499 (1650), Buenos Aires, Buenos Aires, Argentina.
e-mail: perillo@cnea.gov.ar; mariel.atia93@gmail.com;daniel.cnea@gmail.com

ABSTRACT

ZnO nanostructures were synthesized through a chemical method using different Zn precursors and hexamethylenetetramine (HMTA) at 90 °C. The effects of the reactants on the morphological evolution of ZnO nanorods were investigated. The samples were characterized by using XRD, SEM, EDX and BET. The hexagonal wurtzite phase of ZnO was confirmed by X-ray diffraction (XRD). The performed analysis indicated that different morphologies were obtained by changing the reactants.

Keywords: ZnO; crystal growth; nanostructures; chemical synthesis.

RESUMEN

Se sintetizaron nanoestructuras de ZnO por método químico usando diferentes precursores de Zn y hexametilentetraamina (HMTA) a 90 °C y se investigaron los efectos de los reactivos sobre la evolución morfológica de las nanovarillas de ZnO. Las muestras se caracterizaron mediante DRX, SEM, EDX y BET. Se confirmó la fase hexagonal wurtzita para todas las muestras por difracción de rayos x (DRX). Los análisis realizados indican que cambiando los reactivos se obtienen diferentes morfologías.

Palabras clave: ZnO; crecimiento de cristales; nanoestructuras; síntesis química.

1. INTRODUCTION

Recently, many preparation techniques of ZnO nanostructures have been developed, which are classified as physical and chemical methods. Among the physical methods, pulsed laser deposition, magnetron sputtering, electrodeposition, microwave-assisted technique, electron beam evaporation, are found [1–6]. Hydrothermal process, sol–gel, solochemical, chemical vapor deposition, spray pyrolysis and precipitation methods are examples of chemical techniques [7–11]. Physical techniques usually need relatively expensive equipment with high temperatures and high vacuums. Chemical syntheses have some advantages, since they do not need sophisticated equipment with high vacuum level, and therefore they are less expensive. Microstructure of chemically synthesized nanostructures can be precisely controlled by changing the starting materials, temperature, additives, and their concentrations [12–16]. A significant problem of chemical synthesis is the appearance of pollutants and toxic materials that are created as a by-product of the reaction, which hinder the material´s practical and technological applications. Many times the starting materials are toxic and hazardous. There is a great need to develop newer methods and technologies that would make interesting products available through reactions in water or other aqueous media. Chemical techniques with non-toxic materials and at low temperature processing are of great preference [17–19]. In the present work, we synthesized ZnO nanorods by a simple chemistry synthesis from an aqueous solution containing different Zn precursors and HMTA under controlled temperature and without producing pollution waste. The results show that ZnO morphology and the size of the nanorods can be controlled by changing the precursor Zn solution.

2. MATERIALES Y MÉTODOS

2.1 Materials

The zinc acetate dihydrate ($Zn(CH_3COO)_2 \cdot 2H_2O$); zinc chloride ($ZnCl_2$); zinc nitrate hexahydrate ($Zn(NO_3)_2 \cdot 6H_2O$) and hexamethylentetramine (($CH_2)_6N_4$) were of analytical grade and used as received without further purification.

2.2 Synthesis

Three Zn precursors were used: $Zn(CH_3COO)_2 \cdot 2H_2O$; $ZnCl_2$ and $Zn(NO_3)_2 \cdot 6H_2O$. The reactants were first placed in a beaker and mixed during 5 minutes. Then the mixture was placed in a flask attached to a vertical open Liebig condenser in which 100 mL of the Zn precursor and 100 mL of HMTA of equal concentration (0.01M) were heated at 87 °C for 6 h under magnetic stirring. After that, the precipitate was cooled at room temperature, then filtered and washed several times with deionized water and ethanol and finally dried in an oven at 80 °C for 7 h. The ZnO samples obtained from zinc acetate dihydrate, zinc chloride and zinc nitrate hexahydrate were designated *ZnO-Ace, ZnO-Chl* and *ZnO-Nit* respectively.

2.3 Characterization

The morphology of as-synthesized ZnO nanostructures was characterized by scanning electron microscopy (SEM) on a FEI Model Quanta 200, 25 kV microscope combined with an energy dispersive X-ray analyzer (EDX) attached to the SEM. ImageJ software was used to determine the diameter and length of the ZnO nanostructures.

The crystalline structure of the powder was assessed by X-ray diffraction (XRD). The XRD patterns were recorded at room temperature with Cu Kα radiation (λ= 0.15418 nm) in a diffractometer (PANalytical model Empyrean) having theta–theta configuration and a graphite secondary-beam monochromator, using a generator voltage of 40 kV and current of 40 mA. The data were collected for scattering angles (2θ) ranging from 20° to 70° with a step of 0.026° for 2 s per point.

The surface area was calculated using the Brunauer–Emmett–Teller (BET) method based on the adsorption data. The BET specific surface area and pore distribution of the samples were carried out on a Micromeritics Accelerated Surface Area and Porosimetry System ASAP 2020 v 3.01 instrument.

3. RESULTS

3.1 XRD analysis

The X-ray diffraction pattern of ZnO powders are shown in Fig.1. The diffraction peaks at 2θ = 31.7°, 34.3°, 36.2°, 47.5°, 56.5°, 62.7°, 66.2° and 67.8° are identified to be the (100), (002), (101), (102), (110), (103), (200) and (112) reflection planes, respectively. All the indexed peaks in the obtained spectrum are well-matched with the planes of ZnO hexagonal wurtzite structure (01-079-0207). The three diffractograms are very similar. The sharp diffraction peaks indicate the good crystallinity of the prepared samples.
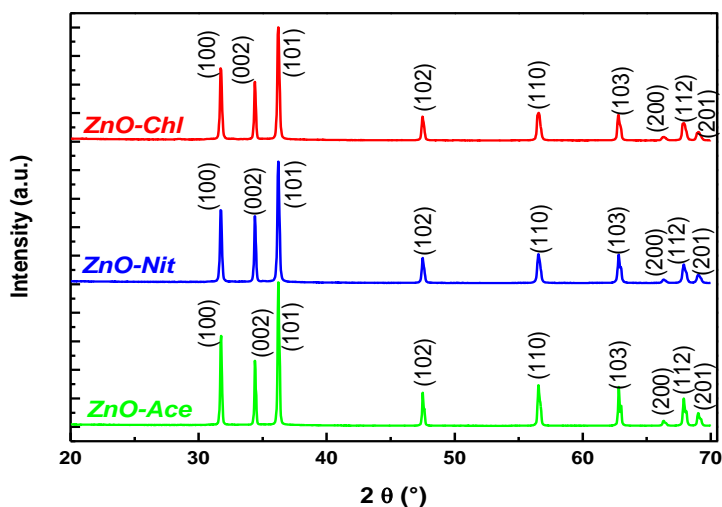

Figure 1: XRD patterns of the ZnO nanorods.

The interplanar spacing (dhkl) calculated from XRD is compared with JCPDS data card, and the percentage of variation of d are summarized in Table 1.

Table 1: Interplanar spacing (dhkl) from XRD, JCPDS data card for corresponding (h k l) planes percentage of variation of d.

hkl	2θ			d_{xrd}			d_{JCPDS}	%$_{variation\ in\ d}$		
	ZnO-Ace	ZnO-Nit	ZnO-Chl	ZnO-Ace	ZnO-Nit	ZnO-Chl	ZnO	ZnO-Ace	ZnO-Nit	ZnO-Chl
(100)	31.78	31.68	31.75	2.8156	2.8243	2.8118	2.8204	-0.170	0.138	-0.304
(002)	34.38	34.31	34.37	2.6084	2.6136	2.6091	2.6062	0.084	0.283	0.111
(101)	36.24	36.14	36.21	2.4787	2.4853	2.4807	2.4806	-0.076	0.189	0.004
(102)	47.47	47.47	47.48	1.9152	1.9152	1.9149	1.9141	0.057	0.057	0.041
(110)	56.59	56.49	56.49	1.6263	1.6289	1.6290	1.6281	-0.110	0.049	0.055
(103)	62.77	62.77	62.77	1.4802	1.4802	1.4802	1.4793	0.060	0.060	0.060

The lattice constants calculated from the XRD data for (100) and (002) planes are shown in Table 2 [20]. The patterns are in accordance with the wurtzite hexagonal structure in the reference data (01-079-0207) and the lattice parameters are similar to the reference data a=b=3.2501Å and c=5.2071Å. No other diffraction peaks are presented, indicating the high purity of the synthesized ZnO products. The Scherrer method for calculating particle size gives an average value of the entire particle responsible for diffraction. The crystallite size is taken to be the size of a coherent diffraction domain and it is not necessarily equal to the particle size.

Table 2: Lattice parameters of the ZnO nanorods.

Sample	a=b (Å)	c (Å)	Average crystal size (nm)
ZnO-Ace	3.251	5.216	46
ZnO-Nit	3.261	5.227	41.3
ZnO-Chl	3.259	5.218	40.6

The orientation degree of ZnO nanostructure can be calculated by the relative texture coefficient Tc, using the following equation, [21]:

$$T_{c(hkl)} = n \frac{I_{(hkl)} / I_{0(hkl)}}{\sum I_{(hkl)} / I_{0(hkl)}}$$

(1)

where $I(hkl)$ and $I_0(hkl)$ are the relative intensity from measured samples and standard sample (01-079-0207), respectively and n is the total number of diffraction peaks considered in the calculation.

We chose six diffractions (n=6) of planes (100), (002), (101), (102), (110) and (103). According to the XRD patterns, the calculated values of Tc (002) were 1.22, 1.30 and 1.21 for **ZnO-Ace**, **ZnO-Nit** and **ZnO-Chl** respectively. The results show that the preferential growth direction is c axis.

Figure 2 shows SEM images of the samples. The images clearly reveal the hexagonal nanorods structure in all cases. The nanorods have an average diameter of ~ 73 nm (**ZnO-Ace**), ~300 nm (**ZnO-Nit**) and ~ 245 nm (**ZnO-Chl**); and lengths up to ~400 nm (**ZnO-Ace**), ~ 1.7µm (**ZnO-Nit**) and ~ 6.5µm (**ZnO-Chl**).
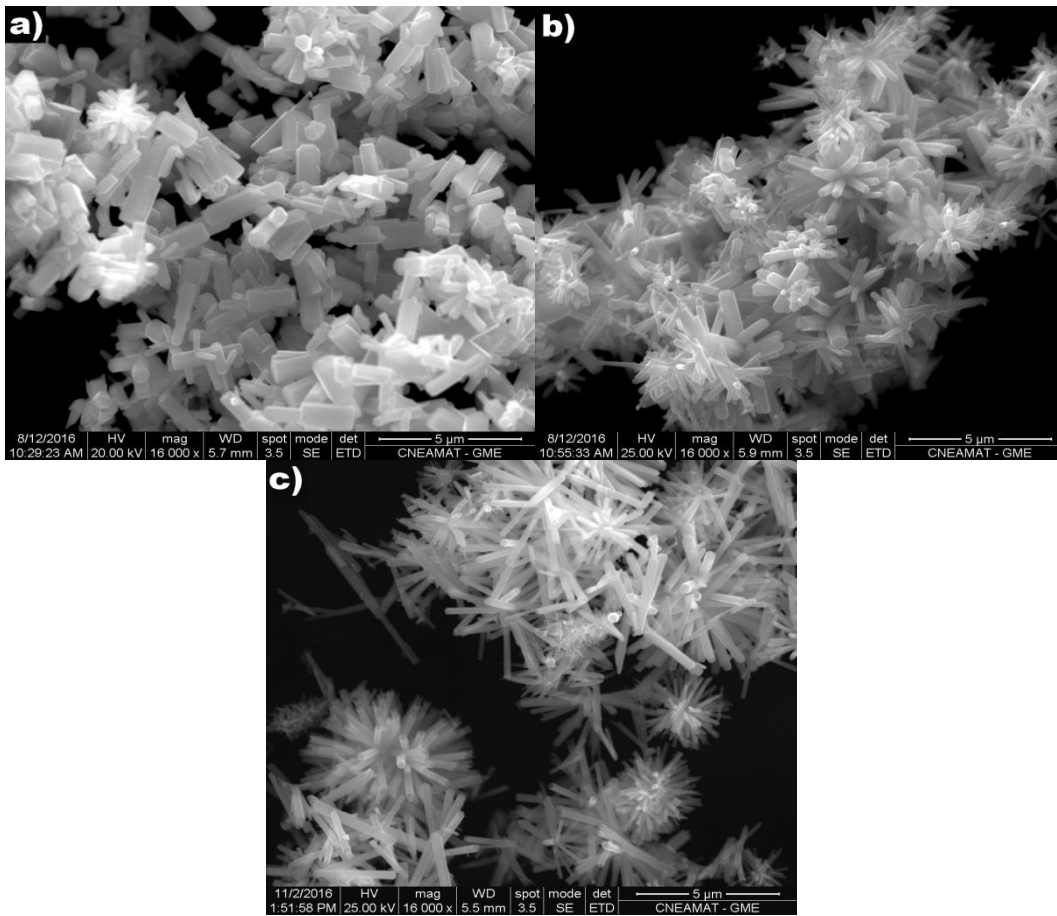
Figure 2: SEM images of ZnO nanorods (a) *ZnO-Ace*; (b) *ZnO-Nit* and (c) *ZnO-Chl*.
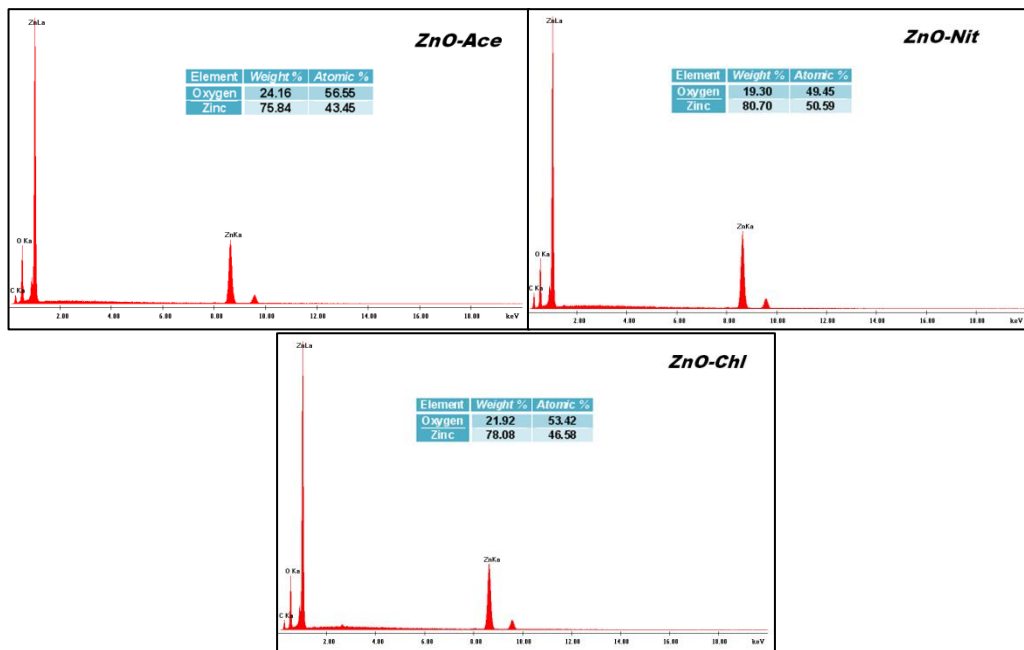

Figure 3: EDX spectra of the nanorods obtained with the three Zn precursors

The surface area and pore volume of the samples were investigated using nitrogen gas adsorption–desorption method. Nitrogen adsorption–desorption isothermal and the corresponding Barrett–Joyner–Halenda (BJH) pore size distribution desorption are presented in Fig. 4. The pore volume distribution curves of ZnO are given as an inset in Figs. 4a, 4b and 4c, respectively. The profiles can be related to type III isotherm with a type III hysteresis loop [22].
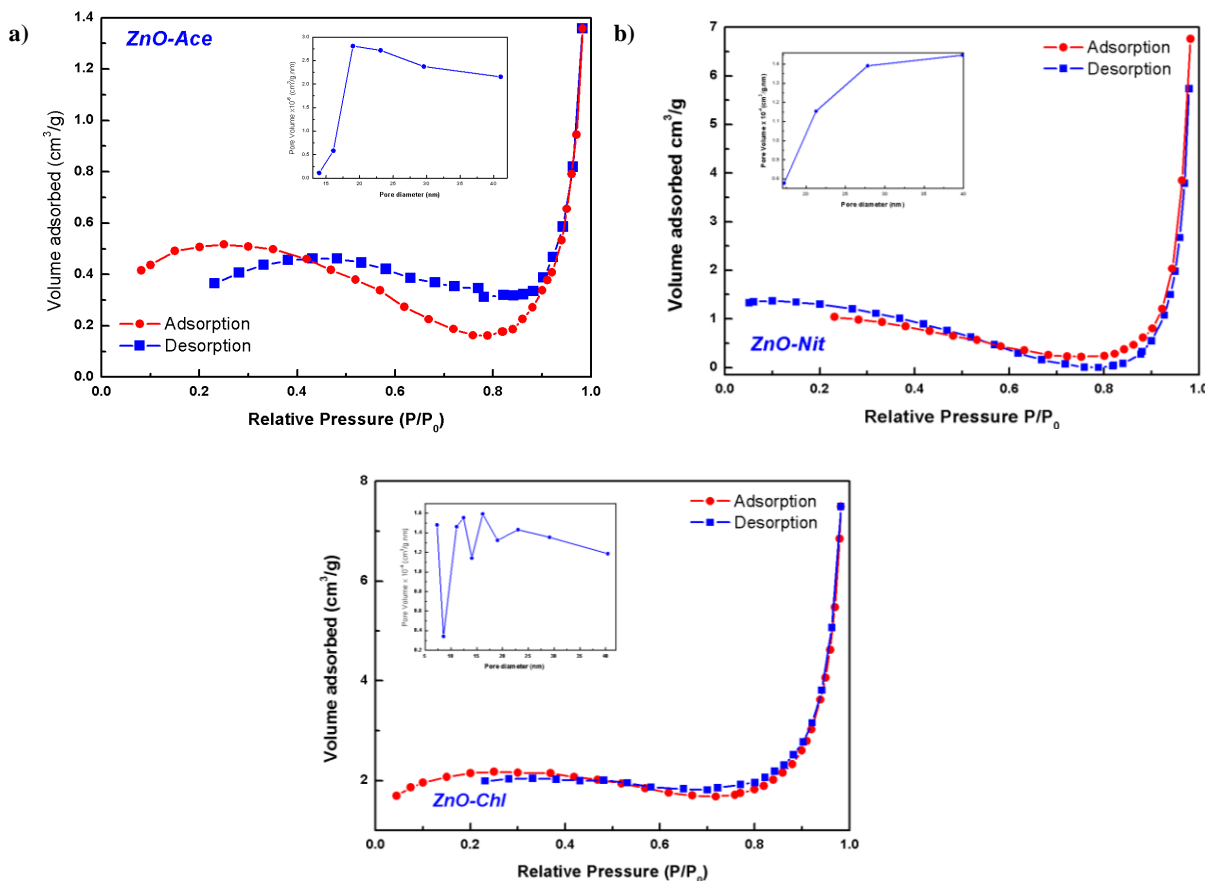

Figure 4: N$_2$ adsorption–desorption isotherms a) ZnO-Ace b) ZnO-Nit and c) ZnO-Chl.

Table 3 shows the results of the measured BET specific surface areas and BJH pore size distributions of the ZnO nanostructures.

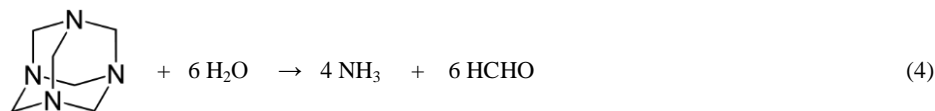**Table 3:** Surface properties of the samples.

Property	ZnO-Ace	ZnO-Nit	ZnO-Chl
BET surface area (m^2/g)	2.01	3.09	7.91
Total pore volume (singlepoint)(cm^3/g)	0.0021	0.0097	0.0116

As it can be seen in Table 3, the **ZnO-Chl** has a higher specific surface area than the other samples probably because of its smaller particle size.

4. DISCUSSION

4.1 The role of HMTA during ZnO crystals growth

The whole reactions most often cited in the literature for white ZnO precipitation are [23]:

$$\text{(HMTA)} \quad + \quad 6\,H_2O \quad \rightarrow \quad 4\,NH_3 \quad + \quad 6\,HCHO \tag{4}$$

$$NH_3 \quad + \quad H_2O \quad \rightarrow \quad NH_4^+ \quad + \quad OH^- \tag{5}$$

$$Zn_2^+ \quad + \quad 4\,OH^- \quad \rightarrow Zn(OH)_4^{2-} \tag{6}$$

$$Zn(OH)_4^{2-} \quad \rightarrow \quad ZnO \quad + \quad 2\,OH^- \quad + 2\,H_2O \tag{7}$$

When the solution is heating up to 87 °C, the HMTA decomposes to form ammonia and formaldehyde [Eq. (4)]. The ammonia reacts with water producing OH^- [eq.(5)]. The Zn^{2+} ions from the precursors reacts with OH^- to form $Zn(OH)_4^{2-}$ complex [Eq.(6)]. The main function of HTMA is to act as pH buffer, slowly releasing OH^-. Finally through thermal decomposition of the $Zn(OH)_4^{2-}$ complex, the white ZnO crystal growth is produced [Eq.(7)]. A similar mechanism has been suggested by Govender et al. [24, 25].

According to the present study, the use of different Zn precursors determines not only the morphology but also the particle size of the final product. This is probably related with the kinetic of the decomposition of the zinc salts in solution. Further systematic studies are required to obtain a quantitative information on the mechanism.

5. CONCLUSIONS

The use of different Zn precursors in the preparation of nanostructured ZnO is an important factor in determining the product morphology. All ZnO samples obtained show rod-like shape, being the only difference the size of the nanorods. When we use Zn Acetate dihydrate as precursor we get short rods and with the use of chloride longer nanorods can be obtained.

6. ACKNOWLEDGEMENT

7. BIBLIOGRAPHY

[1] REN X., ZI W.,WEI Q., LIU S., "Fabrication gallium/graphene core–shell Nanoparticles by pulsed laser deposition and their applications in surface enhanced Raman scattering", *Material Letters,* v.143*,* pp.194–196, march 2015.

[2] SUNDARA VENKATESH, P., DONG, C.L., *et al*., "Local electronic structure of ZnO nanorods grown by radio frequency magnetron sputtering", *Material Letters* v. 116, pp. 206–208, february 2014.

[3] OCAKOGLU K., MANSOUR SH.A., YILDIRIMCAN S., *et al*., "Microwave-assisted hydrothermal synthesis and characterization of ZnO nanorods" *Spectrochimica Acta Part A: Molecular and Biomolecular Spectroscopy*, v. 148, 5, pp. 362–368, september 2015.

[4] CHHIKARA D., SENTHIL KUMAR M., SRIVATSA K.M.K., "On the synthesis of Zn/ZnO core–shell solid microspheres on quartz substrate by thermal evaporation technique", *Superlattice Microstructure* 82 pp. 368–377, june 2015.

[5] VARNAMKHASTI M.G. , FALLAH H. R., ZADSAR M. , "Effect of heat treatment on characteristics of nanocrystalline ZnO films by electron beam evaporation", *Vacuum* v.86, pp. 871–875, february 2012.

[6] MALEKI-GHALEH H., SHAHZADEH M., HOSEINIZADEH S.A., *et al.*, "Evaluation of the photo-electro-catalytic behavior of nano-structured ZnO films fabricated by electrodeposition process", *Materials Letters* v. 169, pp. 140–143, april 2016.

[7] LEE CH-H., KIM D-W., "Thickness dependence of microstructure and properties of ZnO thin Films deposited by metal-organic chemical vapor deposition using ultrasonic nebulization", *Thin solid films* v.546 pp.38–41, november 2013.

[8] GUSATTI M., SOUZA D.A.R, KUHNEN N. C., *et al.*, "Growth of Variable Aspect Ratio ZnO Nanorods by Solochemical Processing", *Journal of Material Science and Technology* v.31, n.1, pp.10–15, january 2015.

[9] FARAG A.A.M., CAVAŞ M., YAKUPHANOGLU F., AMANULLAH F.M., "Photoluminescence and optical properties of nanostructure Ni doped ZnO thin films prepared by sol–gel spin coating technique", *Journal of Alloy and Compound* v. 509 (30), pp. 7900–7908, july 2011.

[10] FABBIYOLA S., KENNEDY L. J., RATNAJI T., *et al.*, "Effect of Fe-doping on the structural, optical and magnetic properties of ZnO nanostructures synthesised by co-precipitation method", *Ceramics International* v. 42(1B), pp. 1588–1596, january 2016.

[11] PETROVIĆ Ž., RISTIĆ M., MARCIUŠ M., *et al.*, "Hydrothermal processing of electrospun fibers in the synthesis of 1D ZnO nanoparticles", *Materials Letters* v. 176, , pp. 278–281, august 2016.

[12] ASTINCHAP, B., MORADIAN, R., NASSERI TEKYEH, M., "Investigating the optical properties of synthesized ZnO nanostructures by sol-gel: The role of zinc precursors and annealing time", *Optik* ,v.127, pp. 9871–9877, october 2016.

[13] LIU T., LI Y., ZHANG H., *et al.*, "Tartaric acid assisted hydrothermal synthesis of different flower-likeZnO hierarchical architectures with tunable optical and oxygen vacancy-induced photocatalytic properties", *Applied Surface science* v. 357, pp. 516–529, december 2015.

[14] EDALATI, K., SHAKIBA, A., VAHDATI-KHAKI, J., *et al.*, "Low-temperature hydrothermal synthesis of ZnO nanorods: Effects of zinc salt concentration, various solvents and alkaline mineralizers" *Materials Research Bulletin* v.74 , pp. 374–379, february 2016.

[15] RAMZAN PARRA M., HAQUE F. Z., "Poly (Ethylene Glycol) (PEG)-Assisted Shape-Controlled Synthesis of One-Dimensional ZnO Nanorods", *Optik – International Journal for Light and Electronic Optic* v. 126, pp. 1562–1566, september 2015.

[16] LI, CH., DU, X., LU, W., *et al.*, "Luminescent single-crystal ZnO nanorods: Controlled synthesis through altering the solvents composition", *Material Letters*, v.81 pp. 229–231, august 2012.

[17] PERILLO P.M., ATIA M.N., RODRÍGUEZ D.F., "Effect of the reaction conditions on the formation of the ZnO nanostructures", *Physica E* v. 85 , pp. 185–192, january 2017.

[18] WANG J., MA P., XIANG L., "Effects of NaOH on formation of ZnO nanorods from ε-Zn(OH)$_2$", *Material Letters* v.141, pp. 118–121, february 2015.

[19] ZHU Y.F., ZHOU G.H., DING H.Y., *et al.*, "Controllable synthesis of hierarchical ZnO nanostructures via a chemical route", *Physica E* , v. 42, pp. 2460–2465, july 2010.

[20] BINDU, P., THOMAS, S. "Estimation of lattice strain in ZnO nanoparticles: X-ray peak profile analysis", *Journal of Theoretical and Applied Physics* v. 8, pp.123–134, december 2014.

[21] KOROTKOV R.Y., RICOU P., FARRAN A.J.E., "Preferred orientations in polycrystalline SnO$_2$ films grown by atmospheric pressure chemical vapor deposition", *Thin Solid Films* v.502, pp. 79–87, 2006.

[22] KIOMARSIPOURN, N., RAZAVI, R. SH., "Hydrothermal synthesis and optical property of scale- and spindle-like ZnO", *Ceramics International* v.39 pp. 813–818, january 2013.

[23] FENG, W., WANG, B., HUANG,P., *et al.*, "Wet chemistry synthesis of ZnO crystals with hexamethylenetetramine (HMTA): Understanding the role of HMTA in the formation of ZnO crystals", *Materials Science in Semiconductor Processing* v. 41, 462–469, January 2016.

[24] GOVENDER K., BOYLE D.S., KENWAY P.B., *et al.*, "Understanding the factors that govern the deposition and morphology of thin films of ZnO from aqueous solution", *Journal of Materials Chemistry* v.14, pp. 2575–2591, june 2004.

[25] ŐZTURK, S., KILINÇ, N., TAŞALTIN, N., *et al.*, "Fabrication of ZnO nanowires and nanorods", *Physica E* v.44 pp.1062-1065, january 2011.